

# Møller polarimetry with atomic hydrogen targets

E. Chudakov<sup>1a</sup> and V. Luppov<sup>2b</sup>

<sup>1</sup> Thomas Jefferson National Accelerator Facility, Newport News, VA23606, USA

<sup>2</sup> University of Michigan Spin Physics Center, Ann Arbor, MI 48109-2036, USA

Received: 15 October 2004 / Published Online: 8 February 2005  
© Società Italiana di Fisica / Springer-Verlag 2005

**Abstract.** A novel proposal of using polarized atomic hydrogen gas, stored in an ultra-cold magnetic trap, as the target for electron beam polarimetry based on Møller scattering is discussed. Such a target of practically 100% polarized electrons could provide a superb systematic accuracy of about 0.5% for beam polarization measurements. Feasibility studies for the CEBAF electron beam have been performed.

**PACS.** 07.60.Fs Polarimeters – 29.25.Pj Polarized targets – 67.65.+z Spin-polarized hydrogen and helium

## 1 Motivation

Precise electron beam polarimetry will become increasingly important for the next generation of parity violation experiments. The systematic errors (polarimetry excluded) and statistical errors of some of these experiments will become better than 0.5%. For example, the measurement of the neutron skin of the <sup>208</sup>Pb nucleus, proposed at Jefferson Lab [1], requires a 1% polarimetry accuracy for the 850 MeV, 50  $\mu$ A polarized electron beam, and would benefit from a polarimetry accuracy of 0.5%.

Compton polarimetry, while accurate enough at the energies  $> 4$  GeV [2, 3] has difficulties at low energies  $\sim 800$  MeV and a 1% accuracy has not been achieved so far.

Møller polarimetry does not depend considerably on the beam energy, but the accuracy is limited by the choice of the polarized electron target. Ferromagnetic foils, used so far, provide electron polarization of about 8%, known either with an accuracy of about 2-3% (see, for example [4, 5, 6]) if the foil is magnetized along its surface in a field of 10-30 mT, or with an accuracy  $\sim 0.3\%$ , if it is magnetized in a very strong field of  $\sim 4$  T [6]. There are other systematic errors, associated with ferromagnetic targets. A kinematics difference in scattering on the external and internal atom shells lead to a systematic error (the so-called Levchuk effect [7]). The target heating limits the beam current to 2-3  $\mu$ A, a factor of 10-30 below the typical currents needed for the experiments. Also, the dead time gives a systematic error.

With all this in mind it seems very attractive to use atomic hydrogen gas, held in an ultra-cold magnetic trap [8], as the source of 100% polarized electrons. Møller polarimetry with such a target would be free of the accuracy limitations discussed above. The target polarization would be close enough to 100% and there will be no need to measure it. There will be no Levchuk effect or noticeable dead time. Here, a feasibility study of such an option is presented.

## 2 Polarized atomic hydrogen target

### 2.1 Hydrogen atom in magnetic field

The magnetic field  $B_S$  and the hyperfine interaction split the ground state of hydrogen into four states with different energies. The low energy states are  $|a\rangle = |\downarrow\uparrow\rangle \cdot \cos\theta - |\uparrow\downarrow\rangle \cdot \sin\theta$  and  $|b\rangle = |\downarrow\downarrow\rangle$ , where the first and second (crossed) arrows in the brackets indicate the electron and proton spin projections on the magnetic field direction. As far as the electron spin is concerned, state  $|b\rangle$  is pure, while state  $|a\rangle$  is a superposition. The mixing angle  $\theta$  depends on the magnetic field  $B_S$  and temperature  $T$ :  $\tan 2\theta \approx 0.05 \text{ T}/B_S$ . At  $B_S = 8$  T and  $T = 0.3$  K the mixing factor is small:  $\sin\theta \approx 0.003$ . State  $|b\rangle$  is 100% polarized. State  $|a\rangle$  is polarized in the same direction as  $|b\rangle$  and its polarization differs from unity by  $\sim 10^{-5}$ .

### 2.2 Storage cell

In a magnetic field gradient, a force  $-\nabla(\mu_H \mathbf{B})$ , where  $\mu_H$  is the atom's magnetic moment, separates the lower and the higher energy states. The lower energy states are pulled into the stronger field, while the higher energy states are repelled from the stronger field. The 0.3 K cylindrical storage cell, made usually of pure copper, is located

<sup>a</sup> This work was supported by the Southeastern Universities Research Association (SURA), which operates the Thomas Jefferson National Accelerator Facility for the United States Department of Energy under contract DE-AC05-84ER40150.

<sup>b</sup> Now with Janis Research Company, Wilmington, MA 01887-0696

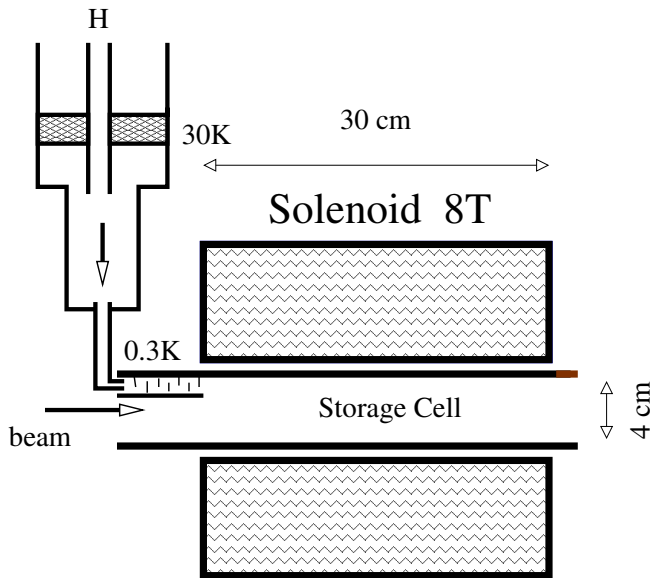


Fig. 1. A sketch of the storage cell

in the bore of a superconducting  $\sim 8$  T solenoid. The polarized hydrogen, consisting of the low energy states, is confined along the cell axis by the magnetic field gradient, and laterally by the wall of the cell (Fig. 1).

At the point of statistical equilibrium, the state population,  $p$  follows the Boltzmann distribution:

$$p \propto \exp(\mu_e B/kT), \quad (1)$$

where  $\mu_e$  is the electron's magnetic moment ( $\mu_H \approx \mu_e$ ) and  $k = k_B$  is the Boltzmann constant. The cell is mainly populated with states  $|a\rangle$  and  $|b\rangle$ , with an admixture of states  $|c\rangle$  and  $|d\rangle$  of  $\exp(-2\mu_e B/kT) \approx 3 \cdot 10^{-16}$ . In the absence of other processes, states  $|a\rangle$  and  $|b\rangle$  are populated nearly equally. The gas is practically 100% polarized, a small ( $\sim 10^{-5}$ ) oppositely polarized contribution comes from the  $|\uparrow\downarrow\rangle$  component of state  $|a\rangle$ .

The atomic hydrogen density is limited mainly by the process of recombination into  $H_2$  molecules (releasing  $\sim 4.5$  eV). The recombination rate is higher at lower temperatures. In gas, recombination by collisions of two atoms is kinematically forbidden but it is allowed in collisions of three atoms. On the walls, which play the role of a third body, there is no kinematic limitation for two atom recombination. At moderate gas densities only the surface recombination matters. In case of polarized atoms, the cross section for recombination is strongly suppressed, because two hydrogen atoms in the triplet electron spin state have no bound states. This fact leads to the possibility of reaching relatively high gas densities for polarized atoms in the traps.

A way to reduce the surface recombination on the walls of the storage cell is coating them with a thin film ( $\sim 50$  nm) of superfluid  $^4\text{He}$ . The helium film has a very small sticking coefficient<sup>1</sup> for hydrogen atoms. In contrast,

<sup>1</sup> The sticking coefficient defines the atom's adsorption probability per a collision with a surface.

hydrogen molecules in thermal equilibrium with the film are absorbed after a few collisions and are frozen in clusters on the metal surface of the trap [9].

The higher energy states are repelled from the storage cell by the magnetic field gradient and leave the cell. Outside of the helium-covered cell, the atoms promptly recombine on surfaces into hydrogen molecules which are either pumped away or are frozen on the walls. Some of the higher energy states recombine within the cell and the molecules eventually are either frozen on the helium-coated wall, or leave the cell by diffusion.

The cell is filled with atomic hydrogen from an RF dissociator. Hydrogen, at 80 K, passes through a Teflon<sup>2</sup> pipe to a nozzle, which is kept at  $\sim 30$  K. From the nozzle hydrogen enters into a system of helium-coated baffles, where it is cooled down to  $\sim 0.3$  K. At 30 K and above, the recombination is suppressed because of the high temperature, while at 0.3 K it is suppressed by helium coating. In the input flow, the atoms and molecules are mixed in comparable amounts, but most of the molecules are frozen out in the baffles and do not enter the cell.

The gas arrives at the region of a strong field gradient, which separates very efficiently the lower and higher atomic energy states, therefore a constant feeding of the cell does not affect the average electron polarization.

This technique was first successfully applied in 1980 [10], and later a density<sup>3</sup> as high as  $3 \cdot 10^{17}$  atoms/cm<sup>3</sup> was achieved [8] in a small volume. So far, the storage cell itself has not been put in a high-intensity particle beam.

For the project being discussed a normal storage cell design can be used, with the beam passing along the solenoid axis (Fig. 1). The double walls of the cylindrical copper cell form a dilution refrigerator mixing chamber. The cell is connected to the beam pipe with no separating windows. The tentative cell parameters are (similar to a working cell [11]): solenoid maximum field of  $B_S = 8$  T, solenoid length of  $L_S = 30$  cm, cell internal radius of  $r_o = 2$  cm, cell length of  $L_C = 35$  cm and temperature of  $T = 0.3$  K. The effective length of such a target is about 20 cm.

For the guideline, we will consider a gas density of  $3 \cdot 10^{15}$  cm<sup>-3</sup>, obtained experimentally [12], for a similar design.

### 2.3 Gas properties

Important parameters of the target gas are the diffusion speed. At 300 mK the RMS speed of the atoms is  $\sim 80$  m/s. For these studies we used a calculated value [13] of the hydrogen atoms cross section  $\sigma = 42.3 \cdot 10^{-16}$  cm<sup>2</sup>, ignoring the difference between the spin triplet and singlet cross sections. This provided the mean free path  $\ell = 0.57$  mm at density of  $3 \cdot 10^{15}$  cm<sup>-3</sup>.

<sup>2</sup> Teflon has a relatively small sticking coefficient for hydrogen atoms.

<sup>3</sup> This parameter is called concentration, but we will use the word density in the text, since the mass of the gas is not important here.

The average time,  $\tau_d$  for a “low field seeking” atom to travel to the edge of the cell, assuming its starting point is distributed according to the gas density, is<sup>4</sup>:  $\tau_d \approx 0.7$  s. This is the cleaning time for an atom with opposite electron spin, should it emerge in the cell and if it does not recombine before. The escape time depends on the initial position of the atom, going from  $\sim 1$  s at  $z = 0$  to 0.1 s at  $z = 8$  cm. The average wall collision time is about 0.5 ms.

## 2.4 Gas lifetime in the cell

For the moment we consider the gas behavior with no beam passing through it. Several processes lead to losses of hydrogen atoms from the cell: thermal escape through the magnetic field gradient, recombination in the volume of gas and recombination on the surface of the cell.

The volume recombination can be neglected up to densities of  $\sim 10^{17}$  cm<sup>-3</sup> [8].

The dominant process, limiting the gas density, is the surface recombination. In order to keep the gas density constant the losses have to be compensated by constantly feeding the cell with atomic hydrogen. Our calculations, based on the theory of such cells [8], show, that a very moderate feed rate of  $\Phi \sim 1 \cdot 10^{15}$  atoms/s would provide a gas density of  $7 \cdot 10^{15}$  cm<sup>-3</sup>.

This can be compared with the measurement [12] of  $3 \cdot 10^{15}$  cm<sup>-3</sup>. The average lifetime of a “high field seeking” atom in the cell is  $\sim 1$  h.

## 2.5 Unpolarized contamination

The most important sources of unpolarized contamination in the target gas in absence of beam have been identified:

- 1) hydrogen molecules:  $\sim 10^{-5}$ ;
- 2) high energy atomic states  $|c\rangle$  and  $|d\rangle$ :  $\sim 10^{-5}$ ;
- 3) excited atomic states  $< 10^{-10}$ ;
- 4) other gasses, like helium and the residual gas in the cell:  $\sim 10^{-3}$

The contributions 1)-3) are present when the cell is filled with hydrogen. They are difficult to measure directly and we have to rely on calculations. Nevertheless, the behavior of such storage cells has been extensively studied and is well understood [8]. The general parameters, like the gas lifetime, or the gas density are predicted with an accuracy better than a factor of 3. The estimates 1)-3) are about 100 times below the level of contamination of about 0.1% which may become important for polarimetry. In contrast, the contribution 4) can be easily measured with beam by taking an empty target measurement. Atomic hydrogen can be completely removed from the cell by heating a small bolometer inside the cell, which would remove the helium coating on this element, and catalyze a fast recombination of hydrogen on its surface. However, it is important

<sup>4</sup> This time was estimated using simulation, taking into account the gas density distribution along  $z$  and the repelling force in the magnetic field gradient.

to keep this contamination below several percent in order to reduce the systematic error associated with the background subtraction.

## 3 Beam impact on storage cell

We have considered various impacts the  $\mathcal{I}_b = 100$   $\mu$ A CEBAF beam can inflict on the storage cell. The beam consists of short bunches with  $\tau = \sigma_T \approx 0.5$  ps at a  $\mathcal{F} = 499$  MHz repetition rate. The beam spot has a size of about  $\sigma_X \approx \sigma_Y \sim 0.1$  mm. The most important depolarization effects we found are:

- A) gas depolarization by the RF electromagnetic radiation of the beam:  $\sim 3 \cdot 10^{-5}$ ;
- B) contamination from free electrons and ions:  $\sim 10^{-5}$ ;
- C) gas excitation and depolarization by the ionization losses:  $\sim 10^{-5}$ ;
- D) gas heating by ionization losses:  $\sim 10^{-10}$  depolarization and a  $\sim 30\%$  density reduction.

The effects A) and B) are described below.

### 3.1 Beam RF generated depolarization

The electromagnetic field of the beam has a circular magnetic field component, which couples to the  $|a\rangle \rightarrow |d\rangle$  and  $|b\rangle \rightarrow |c\rangle$  transitions. The transition frequency depends on the value of the local magnetic field in the solenoid and for the bulk of the gas ranges from 215 to 225 GHz. The spectral density function of the magnetic field can be presented in the form of Fourier series with the characteristic frequency of  $\omega_o = 2\pi\mathcal{F}$ . The Fourier coefficients are basically the Fourier transforms of the magnetic field created by a single bunch. The bunch length is short in comparison with the typical transition frequency ( $\omega_{trans}\tau \sim 0.1$ ). The resonance lines of the spectrum (a reflection of the 499 MHz repetition rate) populate densely the transition range (see Fig. 2). The induced transition rate depends on the gas density at a given transition frequency. This rate was calculated taking into account the beam parameters and the field map of a realistic solenoid. Provided that the field of the solenoid is fine tuned to avoid the transition resonances for the bulk of the gas in the cell (see Fig. 2), the depolarization described has the following features:

- the transition rate is proportional to  $\mathcal{I}_b^2$ ;
- the average rate of each of the two transitions is about  $0.5 \cdot 10^{-4}$  of the target density per second;
- at the center around the beam the full transition rate is about 6% of the density per second.

In order to estimate the average contamination we take into account that each resonance line presented in Fig. 2 corresponds to a certain value of the solenoid field and, therefore, affects the gas at a certain  $z$ . Using a realistic field map of the solenoid we obtained that the average depolarization in the beam area will be reduced to about  $\sim 0.3 \cdot 10^{-4}$  by the lateral gas diffusion and by the escape of the “low field seeking” atoms from the storage cell.

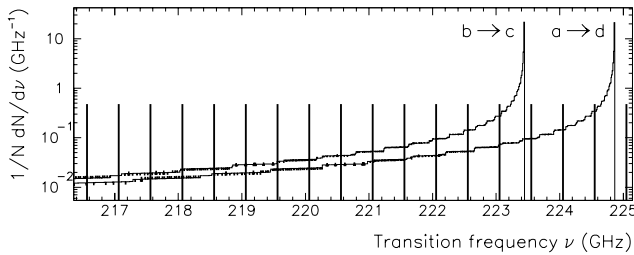


**Fig. 2.** Simulated spectra of the transitions on the axis of the hydrogen trap with the maximum field of 8.0 T. The density of atoms depends on the field as  $\exp(-\mu_e B/kT)$ . The two curves show  $\frac{1}{N} dN/d\nu_{ad}$  and  $\frac{1}{N} dN/d\nu_{bc}$  - the relative number of atoms which can undergo  $|a\rangle \rightarrow |d\rangle$  and  $|b\rangle \rightarrow |c\rangle$  transitions at the given frequency, per one GHz. The resonant structure of the spectral function of the beam-induced electromagnetic field is shown as a set of vertical bars, 499 MHz apart

In order to study experimentally the depolarization effect discussed, one can tune the solenoid magnetic field to overlap a resonance line with the transition frequency of the gas at the cell center. This would increase the transition rate by a factor of  $\sim 70$ .

### 3.2 Contamination by free electrons and ions

The beam would ionize per second about 20% of the atoms in the cylinder around the beam spot. The charged particles would not escape the beam area due to diffusion, as the neutral atoms would do, but will follow the magnetic field lines, parallel to the beam. An elegant way to remove them is to apply a relatively weak  $\sim 1$  V/cm electric field perpendicular to the beam. The charged particles will drift at a speed of  $v = \mathbf{E} \times \mathbf{B}/B^2 \sim 12$  m/s perpendicular to the beam and leave the beam area in about 20  $\mu$ s. This will reduce the average contamination to a  $10^{-5}$  level.

## 4 Application of the atomic target to Møller polarimetry

This feasibility study was done for the possible application of the target discussed to the existing Møller polarimeter in Hall A at JLab [5]. The results are, however, more generic and are largely applicable to other facilities with “continuous” electron beams.

The beam polarization at JLab is normally about 80%, at beam currents below 100  $\mu$ A. Scaling the results of the existing polarimeter to the hydrogen target discussed we estimated that at 30  $\mu$ A a 1% statistical accuracy will be achieved in about 30 min. This is an acceptable time, in particular if the measurements are done in parallel with the main experiment.

There is no obvious way to measure directly the polarization of the hydrogen atoms in the beam area. The contamination from the residual gas is measurable. The rest relies on calculations. All calculations show that the polarization is nearly 100%, with a possible contamina-

tion of  $< 0.01\%$ , coming from several contributions. The impact of the most important of these contributions can be studied, at least their upper limits, by deliberately increasing the effect. For example, the beam RF induced transitions can be increased by a factor of  $\sim 70$ , by fine tuning of the solenoid magnetic field. The contribution from the charged particles in the beam area can be varied by a factor up to  $\sim 10^4$ , by changing the cleaning electric field.

The systematic errors, associated with the present Hall A polarimeter, when added in quadrature give a total systematic error of about 3% [5]. Scaling these errors to the hydrogen target option reduces the total error to about 0.3%.

## 5 Conclusion

The considerations above show that a stored, longitudinally electron-spin-polarized atomic hydrogen can be used as a pure, 100% electron polarized gas target. A thickness of at least  $6 \cdot 10^{16}$  electrons/cm<sup>2</sup> can be reached with a target diameter of 4 cm and a length of 20 cm along the beam. The polarized hydrogen gas should be stable in the presence of a 100  $\mu$ A CEBAF beam. A Møller polarimeter, equipped with such a target would provide a superb systematic accuracy of about 0.5%, while providing a 1% statistical accuracy in about 30 min of running at a beam current of 30  $\mu$ A.

## References

1. C.J. Horowitz, S.J. Pollock, P.A. Souder, R. Michaels: Phys. Rev. C **63**, 025501-1-18 (2001), [arXiv:nucl-th/9912038]
2. M. Baylac et al.: Phys. Lett. B **539**, 8–12 (2002), [arXiv:hep-ex/0203012]
3. M. Woods [SLD Collaboration]: arXiv:hep-ex/9611005
4. P.S. Cooper et al.: Phys. Rev. Lett. **34**, 1589–1592 (1975)
5. A.V. Glamazdin et al.: Fizika B **8**, 91–95 (1999), [arXiv:hep-ex/9912063]
6. M. Hauger et al.: Nucl. Instrum. Methods A **462**, 382–392 (2001), [arXiv:nucl-ex/9910013]
7. L.G. Levchuk: Nucl. Instrum. Methods A **345**, 496–499 (1994)
8. I.F. Silvera, J.T.M. Walraven: “Spin Polarized Atomic Hydrogen,” in *Progress in Low Temperature Physics*, vol. X (Amsterdam: Elsevier Science Publisher B.V., 1986) 139–370
9. I.F. Silvera: Phys. Rev. B **29**, 3899–3904 (1984)
10. I.F. Silvera, J.T.M. Walraven: Phys. Rev. Lett. **44**, 164–168 (1980)
11. T. Roser et al.: Nucl. Instrum. Methods A **301**, 42–46 (1991)
12. M. Mertig, V.G. Luppov, T. Roser, B. Vuaridel: Rev. Sci. Instrum. **62**, 251–252 (1991)
13. M.D. Miller, L.H. Nosanow: Phys. Rev. B **15**, 4376–4385 (1977)